PROBING THE ACTIVE ELECTRON TRANSFER BRANCH IN THE PHOTOSYSTEM I REACTION CENTER FROM *SYNECHOCYSTIS* SP. PCC 6803

Naranbaatar Dashdorj[1], Wu Xu[2], Rachel O. Cohen[3], John H. Golbeck[3,4], Sergei Savikhin[1]. [1]Department of Physics, Purdue University, West Lafayette, IN 47907, USA. [2]Department of Biochemistry, Biophysics, and Molecular Biology, Iowa State University, Ames, IA 50011, USA. [3]Department of Biochemistry and Molecular Biology and [4]Department of Chemistry, The Pennsylvania State University, University Park, PA 16802, USA

Keywords: electron transfer, reaction center, Photosystem I, directionality, cyanobacteria, *Synechocystis* sp. PCC 6803

INTRODUCTION

Photosystem I (PS I) is a pigment-protein complex embedded in the thylakoid membrane that uses the energy of light to reduce ferredoxin or flavodoxin in cyanobacteria, algae and higher plants (Brettel 1997). According to the 2.5 Å crystal structure, the electron transfer chain in PS I is comprised of six chlorophyll (Chl) molecules, two phylloquinones and three [4Fe−4S] clusters (Jordan et al 2001). The Chls and the phylloquinones are arranged in two pseudo-symmetric branches with ligands provided by the PsaA and PsaB protein subunits. The presence of two highly symmetrical branches in the reaction center (RC) raises the question of which branch is active in electron transfer. In this work, point mutations were introduced near the primary electron acceptor sites assigned to A_0 in both the PsaA and PsaB branches of RC in the cyanobacterium *Synechocystis sp.* PCC 6803. The residues $Met688_{PsaA}$ and $Met668_{PsaB}$, which provide the axial ligands to the Mg^{2+} of the eC-A3 and eC-B3 Chls, were changed to leucine and asparagine (Chl notation follows Jordan et al 2001). The removal of the ligand is expected to alter the midpoint potential of the A_0/A_0^- redox pair and affect the kinetics of charge separation. In this work, we studied the dynamics of primary charge separation and secondary electron transfer in these mutants by ultrafast optical pump-probe spectroscopy. Our results suggest that electron transfer in cyanobacterial PS I is asymmetric and occurs primarily along the PsaA branch of cofactors.

MATERIALS AND METHODS

The mutants $M688L_{PsaA}$, $M668L_{PsaB}$, $M688N_{PsaA}$ and $M668N_{PsaB}$ were constructed in *Synechocystis* sp. PCC 6803 by the method described in (Cohen et al 2004). Pump-probe absorption difference profiles (ΔA) were measured using an ultrafast spectrometer described in (Savikhin et al 2000). Samples contained 40 mM sodium ascorbate and 20 μM phenazine methosulfate (PMS) to ensure rapid reduction of $P700^+$. The excitation density was ~1.5 μJ/cm^2 per pulse (1.5 nJ/pulse, ~300 μm spot size), resulting in the excitation of 1 out of every ~1000 Chls. The pump and probe polarizations were separated by 54.7°, to exclude anisotropy effects in the measured kinetics. The (open-closed) absorption difference profiles ($\Delta\Delta A$) were obtained by subtracting kinetics measured for the closed RC from those measured for the open RC. The latter procedure was used to isolate the signal arising from electron transfer processes from that arising from excitation transfer and decay processes (Hastings et al 1995, Savikhin et al 2001).

RESULTS

The formation of the semiquinone state of the secondary electron acceptor A_1 can be monitored directly by its broad near-UV absorption band around 380–390 nm (Brettel & Vos 1999). The time-resolved absorption difference spectra of wild-type PS I with open and closed RCs were recorded at 390 nm after exciting at 660 nm (Fig. 1). Best fit to this profile yielded the intrinsic electron transfer time of 8 to 15 ps for the $A_0^-A_1 \rightarrow A_0A_1^-$ step, which is consistent with our previous results derived from global analysis of (open-closed) profiles (Savikhin et al 2001). The time-resolved (open-closed) profiles measured at 390 nm for PsaB-side mutants were almost superimposable on that of the WT (Fig. 1B), suggesting that the rate of secondary electron transfer is unaffected by the mutations on the PsaB-branch of the RC. However, the A_1^- formation kinetics were dramatically altered in the PS I complexes in which the mutations were introduced on the PsaA-branch of the RC (Fig. 1A). The fits to these (open-closed) profiles revealed that the intrinsic time of the electron transfer from A_0 to A_1 is 112 ± 10 ps and 100 ± 10 ps in the $M688N_{PsaA}$ and $M688L_{PsaA}$ mutants, respectively, which is almost an order of magnitude slower than secondary electron transfer measured in the WT.

According to Savikhin et al (2001), the (open-closed) $\Delta\Delta A$ profile probed at 690 nm closely follows the dynamics of formation and

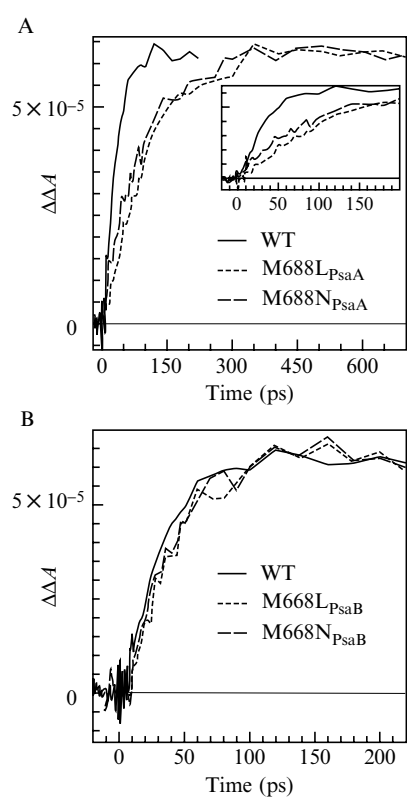

Figure 1: Time-resolved (open-closed) absorption difference profiles for WT, $M688L_{PsaA}$ and $M688N_{PsaA}$ mutants (A), and for WT, $M668L_{PsaB}$ and $M668N_{PsaB}$ mutants (B). All samples were excited at 660 nm and absorption differences were probed at 390 nm.

decay of the A_0^- state. At this particular wavelength, the initial rise of PB is primarily due to the formation of the A_0^- state, since the $(A_0^- - A_0)$ spectrum has a maximum PB at ~686 nm (Hastings et al 1994, Savikhin et al 2001). Figure 2B shows the (open-closed) $\Delta\Delta A$ profile measured at 690 nm for PS I complexes from the WT (Savikhin et al 2001) and the $M668L_{PsaB}$ and $M668N_{PsaB}$ mutants. The only change in the case of the PsaB-side mutants is the level of the residual absorption, which is consistent with the lower ($P700^+ - P700$) absorption level measured at 690 nm in the mutants (data not shown). A simple two-exponential fit to the $\Delta\Delta A$ profiles reveals a ~10 ps PB rise followed by a ~24 ps PB decay for all three curves, suggesting that the PsaB-side mutations do not affect ET. As in the case of the 390 nm pump-probe profiles, dramatic differences were observed in the $\Delta\Delta A$ signals measured for the PsaA-side mutants at 690 nm (Fig. 2A, notice the time-scale change). Biexponential fits to these profiles reveal ~11.4 ps and ~10.4 ps PB rise times, combined with 130 ± 20 ps and 145 ± 20 ps PB decay times for the $M688L_{PsaA}$ and $M688N_{PsaA}$ mutants, respectively. The longer PB decay at 690 nm observed for the PsaA-side mutants reflects a longer $A_0 \rightarrow A_1$ ET time, and is consistent with the pump-probe data obtained at 390 nm.

Absorption difference kinetics for PS I complexes with open RC from all mutants were probed in the range of 650–720 nm and analyzed globally to produce decay-associated spectra (DAS) as described in (Savikhin et al 2000). The pump-probe profiles for PS I complexes from the PsaB-side mutants could be described by four DAS components which closely resembled DAS measured for complexes from the WT (Savikhin et al 2000). Global fits to the pump-probe profiles obtained for PS I complexes from the PsaA-side mutants were only possible with the addition of a fifth 100–200 ps component. The DAS of this additional component had a fwhm of 11–15 nm and was centered at 689 ± 1 and 684 ± 1 nm in the case of PS I complexes from the $M688L_{PsaA}$ and $M688N_{PsaA}$ mutants, respectively (not shown). Its spectral shape and magnitude are consistent with the PB spectrum of a single Chl *a* molecule, and we attribute this component to the decay of the A_0^- state, which reflects electron transfer from A_0^- to A_1.

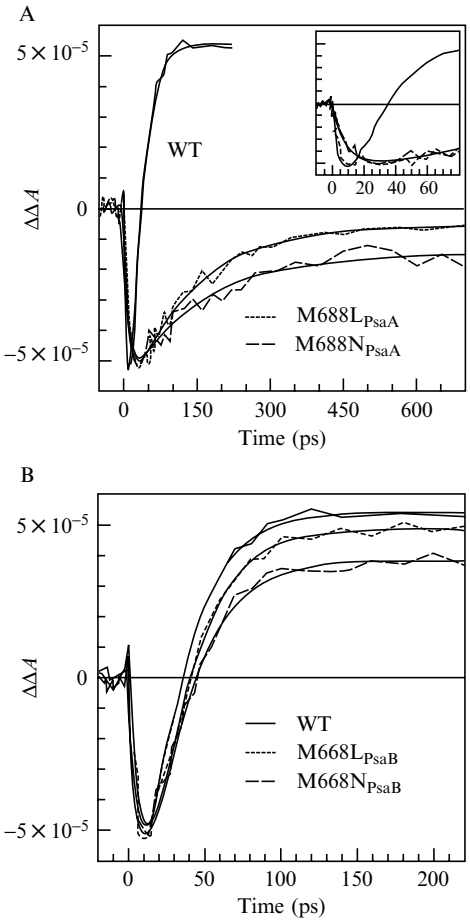

Figure 2: Time-resolved (open-closed) absorption difference profiles for WT, $M688L_{PsaA}$ and $M688N_{PsaA}$ mutants (A), and for WT, $M668L_{PsaB}$ and $M668N_{PsaB}$ mutants (B). All samples were excited at 660 nm and absorption differences were probed at 690 nm.

DISCUSSION

The results reported in this work indicate that mutations on the PsaA-branch of cyanobacterial PS I markedly alter the kinetics of the first steps of electron transfer as well as the spectral properties of the primary electron acceptor A_0, whereas mutations on the PsaB-branch maintain kinetics and spectral properties that are essentially undistinguishable from the WT. The secondary electron transfer $P700^+A_0^-A_1 \rightarrow P700^+A_0A_1^-$ occurs with an intrinsic time of 100–150 ps in the $M688L_{PsaA}$ and $M688N_{PsaA}$ mutants, which is 3–10 times slower than the secondary electron transfer step reported for the WT (Brettel & Leibl 2001, Savikhin et al 2001). We considered three possible scenarios to explain this effect: (i) in wild-type PS I complexes ET occurs concurrently along both branches, but the mutation near A_0 blocks the ET along the respective RC branch, and the observed ET rate difference in the PsaA- and PsaB-branch mutants is due to different ET rates along PsaA- and PsaB-branches in wild-type PS I; (ii) in the WT and PsaB-side mutants ET occurs primarily along the PsaA-branch and mutations in the latter redirect ET to the PsaB-branch; (iii) ET always occurs primarily along the PsaA-branch and its rate is affected by mutations near A_0. According to our detailed analysis the scenario (i) fails to describe experimental data. Scenario (ii) could explain the observed kinetics only in the assumption that mutations in the PsaA branch can affect the spectral properties of the A_0 pigment in the opposite branch. The results of our experiments are best consistent with the scenario (iii). Thus, our results provide additional evidence for asymmetric ET in cyanobacterial PS I, which was previously suggested by Cohen et al (Cohen et al 2004). According to our data, at least 80% of the electrons transferred in these RCs proceed along the PsaA-branch. These results contrast with the finding that electron transfer in PS I from several eukaryotes proceeds with almost equal probability along both branches of the RC. Our results also indicate that the relatively small changes in PS I protein structure expected for these mutations may have a significant impact on the electron transfer process.

ACKNOWLEDGMENTS

This work was supported by a grant from the National Science Foundation (MCB-0117079), and Purdue Research Foundation grant 6903680.

© 2005 by the International Society of Photosynthesis

REFERENCES

Brettel, K. (1997) *Biochim. Biophys. Acta* 1318: 322–373.

Brettel, K. & Leibl, W. (2001) *Biochim. Biophys. Acta* 1507: 100–114.

Brettel, K. & Vos, M. H. (1999) *FEBS Lett.* 447: 315–317.

Cohen, R. O., Shen, G., Golbeck, J. H., Xu, W., Chitnis, P. R., Valieva, A. I., van der Est, A., Pushkar, Y. & Stehlik, D. (2004) *Biochemistry* 43: 4741–4754.

Hastings, G., Hoshina, S., Webber, A. N. & Blankenship, R. E. (1995) *Biochemistry* 34: 15512–15522.

Hastings, G., Kleinherenbrink, F. A. M., Lin, S., McHugh, T. J. & Blankenship, R. E. (1994) *Biochemistry* 33(11): 3193–3200.

Jordan, P., Fromme, P., Witt, H. T., Klukas, O., Saenger, W. & Krauss, N. (2001) *Nature* 411: 909–917.

Savikhin, S., Xu, W., Chitnis, P. R. & Struve, W. S. (2000) *Biophys. J.* 79: 1573–1586.

Savikhin, S., Xu, W., Martinsson, P., Chitnis, P. R. & Struve, W. S. (2001) *Biochemistry* 40: 9282–9290.

ANTENNA RING AROUND TRIMERIC PHOTOSYSTEM I IN CHLOROPHYLL *b*-CONTAINING CYANOBACTERIUM *PROCHLOROTHRIX HOLLANDICA*

Ladislav Bumba[1,2], Ondřej Prášil[3,4], František Vácha[2,4]. [1]Faculty of Biological Sciences, University of South Bohemia, České Budějovice, Czech Republic. [2]Institute of Plant Molecular Biology, Czech Academy of Sciences, České Budějovice, Czech Republic. [3]Institute of Physical Biology, University of South Bohemia, Nové Hrady, Czech Republic. [4]Institute of Microbiology, Department of Autotrophic Microorganisms, Třeboň, Czech Republic

Keywords: photosystem I, *Prochlorothrix hollandica*, chlorophyll *a/b* antenna protein, electron microscopy, single particle image analysis

INTRODUCTION

The freshwater phytoplankton *Prochlorothrix hollandica* is filamentous cyanobacterium which has been recently found in the shallow eutrophic lakes in the Netherlands (Burger-Wiersma et al 1986). *Prochlorothrix*, as well as *Prochloron* and *Prochlorococcus* species belongs to an unusual group of cyanobacteria (formerly called Prochlorophyta) which do not collect the light radiation energy required for photosynthetic processes as the usual cyanobacteria by means of water-soluble phycobilisomes, however instead of that they use intrinsic light-harvesting proteins that bind chlorophyll *a* and *b* molecules (Partensky & Garczarek 2003). The Chl *a/b*-binding proteins (encoded by *pcb* genes) are predicted to have six transmembrane helices and thus, they are not phylogenetically related to the *cab* genes encoding a superfamily of the widely spread light-harvesting antenna proteins of green plastids. Instead, they are similar to the iron-stress induced *is*iA gene product of cyanobacteria and to the CP43 protein, a constitutively expressed Chl *a* inner antenna protein of photosystem II (LaRoche et al 1996). In *P. hollandica* three Pcb antenna proteins (*pcb*A–C gene products) are organized in tandem and are cotranscribed (van der Staay et al 1998). Here we present a structural study of *P. hollandica* that complement the overall view on organization of light-harvesting antennae complexes of photosystem I (PSI) in prochlorophyta family showing a ring-like structure around PSI as an unique mechanism significantly increasing the size of the light-harvesting antenna system in unfavorable dark conditions.

MATERIALS AND METHODS

The cells of *Prochlorothrix hollandica* (SAG 10.89) were grown in BG11 medium under continuous illumination at an irradiation level of 20 μmol photons $m^{-2} s^{-1}$ at 20 °C. Thylakoid membranes were isolated according to van der Staay and Staehelin (1994), instead of the cells were broken with glass beads in a *Beadbeater* cell homogenizer. The thylakoid membranes were solubilized by β-dodecyl-maltoside and subjected to a sucrose density gradient centrifugation. The biochemical characterization of the gradient bands were conducted according to Bumba et al (2004). The lowest green band of the sucrose gradient was applied on glow-discharged carbon coated grid and negatively stained with 2% uranyl acetate. Electron microscopy was performed with a Philips TEM 420 at magnification of 60.000×. The obtained images were then processed with SPIDER image analysis workpackage (Frank et al 1996). For the molecular modeling, the coordinates were taken from Protein Data Bank (www.rcsb.org/pdb) under the code 1JB0 for PSI 2.5 Å structure (Jordan et al 2001).

RESULTS

Sucrose density gradient centrifugation of *P. hollandica* thylakoid membranes solubilized with β-dodecyl-maltoside resulted in the separation of six green bands (band 1–6, Fig. 1A). All the bands were characterized by their protein composition, absorption and 77 K fluorescence emission spectra and by HPLC size exclusion chromatography. These results clearly indicated that bands 1 and 2 consisted mainly of Pcb antenna proteins and the bands 3 and 5 corresponded to monomeric and trimeric photosystem I (PSI), respectively. The lowest green band 6 was also enriched in polypeptides of the PSI reaction center complex, such as the PsaA/B reaction center proteins and lower molecular weight subunits of PSI (PsaC, PsaD, PsaE, PsaF, PsaK, PsaL) as well as this band was associated with the Pcb proteins (Fig. 1B, lane 6).

Room temperature absorption spectrum of the band 6 exhibited absorption maximum in the red region at 673 nm (Fig. 1C). The red peak is blue-shifted as compared to the PSI trimers absorbing at 680 nm and this shift is due to the presence of the Pcb proteins, which absorbs at 671 nm. The 77 K fluorescence emission spectrum of the band 6 showed two emission peaks with two maxima at 685 nm and 720 nm (Fig. 1D) corresponding to free Pcb proteins and to PSI, respectively. Since free Pcb subunits were highly fluorescent with the maximum at 685 nm, then it can be concluded that in this band, a small portion of free Pcb subunits were presented as contaminants.

In order to reveal how Pcb proteins interact with PSI the band 6 was negatively stained with uranyl acetate and subjected to electron microscopy. A typical electron micrograph in Fig. 2A shows that the band 6 contained a mixture of several types of particles.